Crystal Structure of NAD(P)H:Flavin Oxidoreductase from *Escherichia coli*[†,‡]

Margareta Ingelman,[§] S. Ramaswamy,[§] Vincent Nivière,[||] Marc Fontecave,*[,||] and Hans Eklund*[,§]

Department of Molecular Biology, Swedish University of Agricultural Sciences, Biomedical Center, Box 590, S-751 24 Uppsala, Sweden, and Laboratoire de Chimie et Biochimie des Centres Rédox Biologiques, DBMS-CEA/CNRS/Université Joseph Fourier, 17 Avenue des Martyrs, 38054 Grenoble Cedex 9, France

Received December 3, 1998; Revised Manuscript Received March 16, 1999

ABSTRACT: Flavin reductases use flavins as substrates and are distinct from flavoenzymes which have tightly bound flavins. The reduced flavin can serve to reduce ferric complexes and iron proteins. In *Escherichia coli,* reactivation of ribonucleotide reductase is achieved by reduced flavins produced by flavin reductase. The crystal structure of *E. coli* flavin reductase reveals that the enzyme structure is similar to the structures of the ferredoxin reductase family of flavoproteins despite very low sequence similarities. The main difference between flavin reductase and structurally related flavoproteins is that there is no binding site for the AMP moiety of FAD. The direction of the helix in the flavin binding domain, corresponding to the phosphate binding helix in the flavoproteins, is also slightly different and less suitable for phosphate binding. Interactions for flavin substrates are instead provided by a hydrophobic isoalloxazine binding site that also contains a serine and a threonine, which form hydrogen bonds to the isoalloxazine of bound riboflavin in a substrate complex.

Free reduced flavins, FAD and FMN but also riboflavin, have been suggested to have important biological functions as electron-transfer mediators, even though the real physiological significance of these mediators has so far not been fully appreciated (*1*). Reduced flavins serve to reduce ferric complexes or iron proteins with low redox potential. For example, by reducing ferrisiderophores in microorganisms, they participate in key steps of iron uptake and metabolism (*1*). In prokaryotes, reduced flavins were suggested to participate in the regulation of deoxyribonucleotide synthesis by reducing the iron center of ribonucleotide reductase and in the repair of its essential tyrosyl radical (*2*−*5*). In human erythrocytes, reduced flavins may also reduce methemoglobin efficiently, explaining why methemoglobinemia can be treated successfully with riboflavin (*6*−*8*). This genetic disease is characterized by an inactive cytochrome b_5 reductase, the physiological methemoglobin reductase.

A number of enzyme systems, consisting of an oxygenase with the ability to use the reduced flavin/molecular oxygen combination in the form of a flavin hydroperoxide as an oxidant source, have been characterized. The first example of such an oxidizing system was found in the bioluminescent bacteria *Vibrio harveyi* (*9*). These microorganisms contain a luciferase enzyme system which catalyzes the oxidation of a long-chain aliphatic aldehyde by oxygen in the presence of a reduced flavin. This reaction, which is responsible for light emission, implies a flavin hydroperoxide intermediate stabilized by the enzyme. Such activities have been found in *Streptomyces* species for oxidation steps during the biosynthesis of antibiotics, such as actinorhodin, pristamycin, or valanimycin (*10*−*12*), and in *Chelatobacter heintzii* to be used for degradation of nitrilotriacetate (*13*). *Rhococcus* has been shown to use a similar system, encoded by the *dsz* genes, to oxidize sulfides into sulfoxides and sulfones, allowing the utilization of these microorganisms in an original fossil fuel desulfurization biotechnological process (*14*).

The nonenzymatic reduction of free flavins by NADPH or NADH is slow (*15*), and as a consequence, living organisms have evolved enzymes that catalyze the reduction of riboflavin, FMN, and FAD by NADPH or NADH which are called NAD(P)H:flavin oxidoreductases or flavin reductases (*2*). They do not contain a flavin as a prosthetic group and thus cannot be classified as flavoproteins. Instead, they use flavins as substrates, with a rather broad substrate specificity (*16*). The catalysis of the reaction is made possible through the existence of a site which accommodates both reduced pyridine nucleotide and the flavin substrate (*17*).

There are several subgroups of flavin reductases as shown from the variety of nonhomologous amino acid sequences. One, named Fre, is found in *Escherichia coli* and the luminous bacteria, *V. harveyi, Vibrio fischeri, Vibrio orientalis,* and *Photorhabdus luminescens.* A second protein, LuxG, was found in the lux operons of these bacteria. LuxG shows significant sequence homology to Fre and has a comparable molecular weight (Figure 1). Fre, LuxG, and a flavoprotein with flavin reductase activity are all suspected to be involved in the bioluminescent process in *V. harveyi.* The enzymes involved in antibiotics synthesis show no homology to Fre and may comprise a separate group of flavin reductases.

[†] This work was supported by grants from Swedish Natural Science Research Council and NUTEK (to H.E.).

[‡] The atomic coordinates described in this paper have been deposited in the Brookhaven Data Bank (entry 1qfj).

* To whom correspondence should be addressed. Telephone: 46-18 471 45 59. Fax: 46-18 53 69 71. E-mail: hasse@xray.bmc.uu.se.

[§] Swedish University of Agricultural Sciences.

[||] DBMS-CEA/CNRS/Université Joseph Fourier.

10.1021/bi982849m CCC: $18.00
Published on Web 05/08/1999

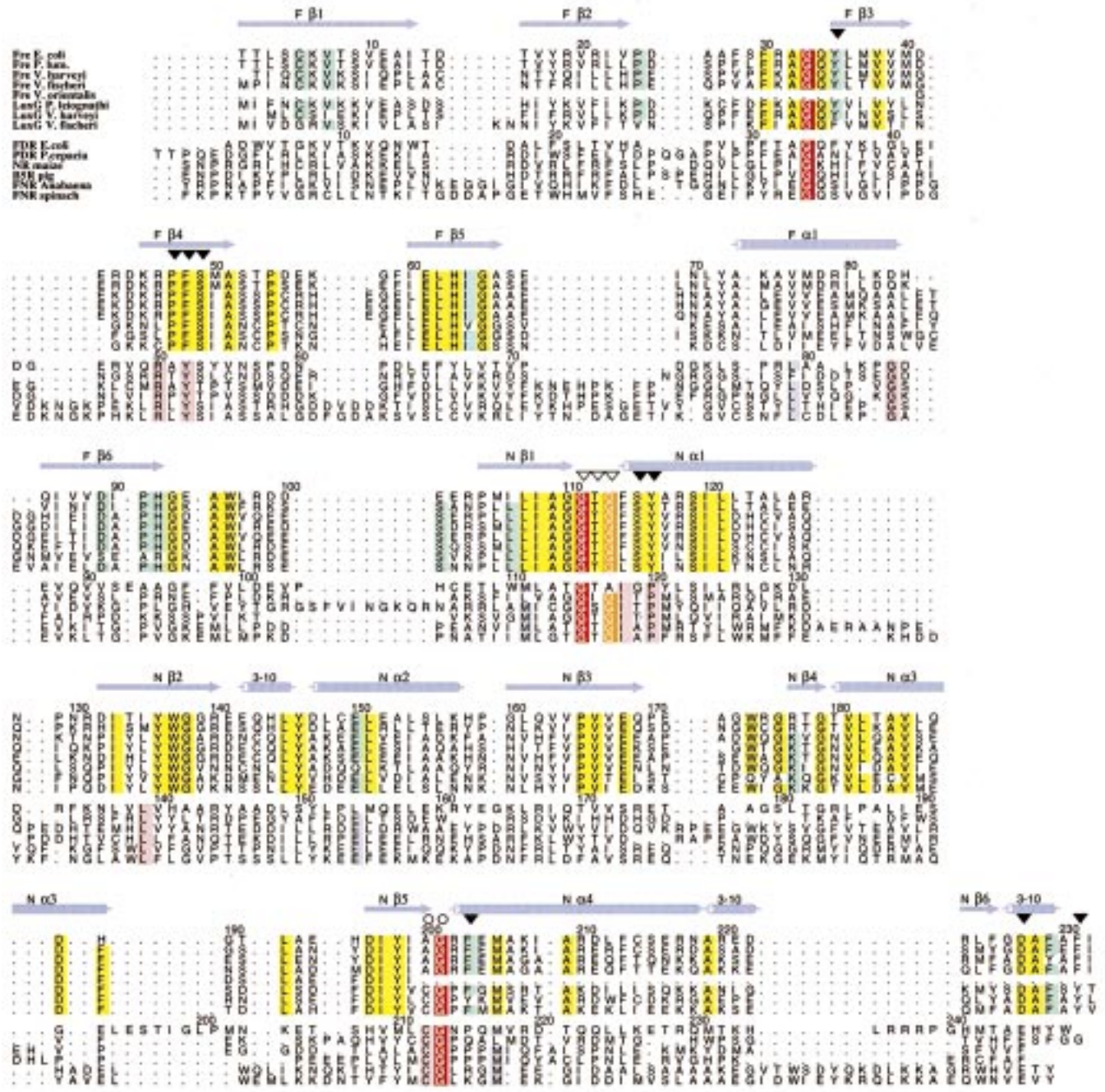

FIGURE 1: Sequence homology between different flavin reductases of the Fre and LuxG family and between members in the ferredoxin reductase superfamily which are aligned according to the superimposed three-dimensional structure. The secondary structure elements are numbered consecutively within each domain with the prefix F and N, respectively. Residues conserved within the Fre/Lux family are shown in yellow and those which differ by one residue are in light green. Completely conserved residues within the superfamily are shown in red and those that differ by one residue are in orange. Residues conserved in the superfamily but excluding the Fre/Lux family are colored pink while those that differ by one residue are in light blue. Filled triangles above the sequences mark riboflavin binding residues, open triangles mark the Gly fingerprint of the α/β domain, and open circles mark residues probably located at the nicotinamide binding site. The sequence identities between *E. coli* flavin reductase and other flavin reductases of the Fre and Lux type are as follows: Fre from *P. luminescens* 73%, Fre from *V. harveyi* 48%, Fre from *V. fischeri* 51%, Fre from *V. orientalis* 52%, LuxG from *Photobacterium leiognathi* 36%, LuxG from *V. harveyi* 48%, and LuxG from *V. fischeri* 41%.

The most extensively studied of these systems so far is the Fre enzyme from *E. coli*, the prototype of flavin reductases (*2*, *16*−*18*). It consists of a single polypeptide chain of 232 amino acids and a molecular mass of 26 kDa. It uses both NADPH and NADH as the electron donor and a great variety of flavin analogues as electron acceptors, demonstrating that the recognition of the flavin by the polypeptide chain occurs exclusively through the isoalloxazine ring, with very limited contribution to the binding by the ribityl side chain. The flavin reductase gene has been cloned (*18*), and the amino acid sequence is shown in Figure 1.

In this paper we report the first structure of a flavin reductase of the Fre type. The three-dimensional structure of flavin reductase has been determined at 2.2 Å resolution. The most remarkable finding is the extensive structural homology with a class of flavoprotein enzymes which includes the structurally characterized ferredoxin−$NADP^+$

Table 1: Data Collection and Phasing Statistics

data set	wavelength (Å)	I/σ	resoln (Å)	compl (%)	total no. of refl	no. of unique refl	R_{fac}[a] (%)	no. of sites	phasing power[b] acentric refl iso	phasing power[b] acentric refl ano	Cullis R-factor[c] acentric refl iso	Cullis R-factor[c] acentric refl ano
λ1 KAu(CN)2(peak)	1.0392	11.5	2.6	98.0 (99.3)	140 153	34 497	5.0	10	1.68	2.04	0.59	0.76
λ2 KAu(CN)2(infl.)	1.03964	11.3	2.6	98.1 (99.5)	139 956	34 537	5.1	10	2.18	1.85	0.49	0.81
λ3 KAu(CN)2(remote)	0.9536	11.3	2.6	96.2 (92.8)	137 588	33 896	5.2	10	0	1.73	0	0.84
native		9.3	2.2	93.2 (88.2)	626 153	54 692	6.4					
highest shell Au 2.60−2.74												
highest shell native 2.20−2.24												
$FOM_{SHARP} = 0.549$												
$FOM_{DM} = 0.722$												

[a] $R_{fac} = \sum\sum_i|I_i - \langle I\rangle|/\sum|\langle I\rangle|$. [b] Phasing power = F_H/E or $\langle F_H\rangle$/(lack of closure). [c] $R_{Cullis} = \sum||F_{PH} + F_P| - |F_H\ (calc)||/\sum|F_{PH} - F_P|$ or R_{Cullis} is ⟨lack of closure⟩/⟨isomorphous difference⟩.

reductase, FNR (*19*−*23*), cytochrome b_5 reductase (*24*, *25*), nitrate reductase (*26*, *27*), phthalate dioxygenase reductase, PDR (*28*, *29*), flavodoxin reductase (*30*), and cytochrome P-450 reductase (*31*), although the overall sequence similarity is less than significant.

MATERIALS AND METHODS

Purification. Flavin reductase was prepared from *E. coli* cells as previously described (*16*). To obtain crystals, an additional step on a 5/5 MonoQ column (Pharmacia Biotech) was conducted. Protein (2−4 mg) was applied at low ionic strength in a 25 mM Tris-HCl buffer at pH 7.6 containing 10% glycerol and then eluted with a shallow gradient of 0.1−0.2 M NaCl. This gave rise to two or more peaks of isoforms of flavin reductase. Only the top fractions of the major peak were pooled, concentrated, and used for crystallization experiments.

Crystallization. Crystallization of the flavin reductase was carried out in vapor diffusion systems using Falcon microtitration plates. Droplets (2−4 μL) of protein solution (15 mg/mL of protein) were mixed with an equal amount of the buffered precipitation mixture. Several different crystal forms were obtained under quite similar conditions, and three of them have been crystallographically characterized. All crystal forms were grown at 4 °C from PEG 4000 containing 0.5−1 M NaCl with only slight variations of pH and concentration of precipitant. Two of the crystal types are tetragonal, and a third orthorhombic crystal form has cell dimensions related to the others. The data used for the structure determination were obtained from the orthorhombic $P2_12_12_1$ crystal. They appeared in 15−20% PEG 4000 (Supelco), 0.5 M NaCl, and 100 mM Bis-tris propane, pH 6.5. The crystals contain four molecules per asymmetric unit and have a solvent content of 51%. For binding studies, orthorhombic crystals were soaked in 0.1 mM riboflavin.

Data Collection. A native data set to 2.2 Å was collected at the BW7B beamline (EMBL, DESY, Hamburg). This crystal had the cell dimensions $a = 51.3$ Å, $b = 97.0$ Å, and $c = 211.2$ Å. A total of 297 frames were collected with 0.8° oscillation. The data were processed using DENZO and scaled in SCALEPACK (HKL software package) (*32*).

The structure was solved by the multiple anomalous diffraction method (MAD). Crystals were soaked in 4 mM $KAuCN_2$ overnight and then back-soaked for a few minutes into the mother liquor containing the cryo solution (20% PEG 400, 20% PEG 4000, 0.5 M NaCl, and 100 mM Bis-tris propane, pH 6.5). An EXAFS scan of the crystals in the BM14 beam line at Grenoble clearly indicated that there was gold in the crystals. The EXAFS scan was used to identify and define a peak (1.0392 Å), inflection point (1.03964 Å), and a remote wavelength (wavelength 0.9536 Å). A total of 101 frames of data on each wavelength with 1° oscillation were collected. The data were good at 2.8 Å resolution and were collected one wavelength after the other. Details are given in Table 1.

Of the total 33 896 unique independent reflections, 29 773 are acentric and anomalous measurements were made for 29 535 of them. The overall redundancy is over 4.0. Of the total number of reflections collected (140 237), over 139 636 have an $I/\sigma I$ greater than 1.0. The mean $I/\sigma I$ is 12.0.

Structure Determination. An anomalous difference Patterson map was calculated using the programs in the CCP4 suite (*33*). This clearly revealed the position of the first two sites which were input to SHARP (*34*). A total of 10 sites were found from the residual maps calculated by SHARP. The final R_{Cullis} varied from 0.49 to 0.66 and the phasing power from 2.1 to 1.6 for the various isomorphous and anomalous differences. The mean figure of merit was 0.56 (0.40) for acentric reflections and 0.46 (0.28) for centric reflections (mean figure of merit between 2.78 and 2.6 Å resolution is shown in parentheses).

The map calculated with these phases was reasonably good, and it was easy to see the protein and the solvent regions. SOLOMON (*35*) was used to improve the phases, and with 45% solvent the mean figure of merit was 0.88 (0.81 between 2.78 and 2.6 Å resolution). The polypeptide chain could easily be traced in this map. An averaged map (*36*) was used in the initial stages.

The structure was built using the program O (*37*) and refined using the program REFMAC (*38*). After a reasonably well refined model was obtained, molecular replacement with Amore (*39*) was used to determine the position of the molecule in the native data, which is of much higher resolution.

Refinement. The structure was refined further with REFMAC to an R-factor of 23.2% and an R_{free} of 29.6% for all data between 20.0 and 2.2 Å resolution. Refinement was carried out with NCS restraints placed on both coordinates and on B-factors. Waters were picked automatically using the program ARP (*40*) and were later examined on the graphics using O (*37*). The rms deviations of bond lengths

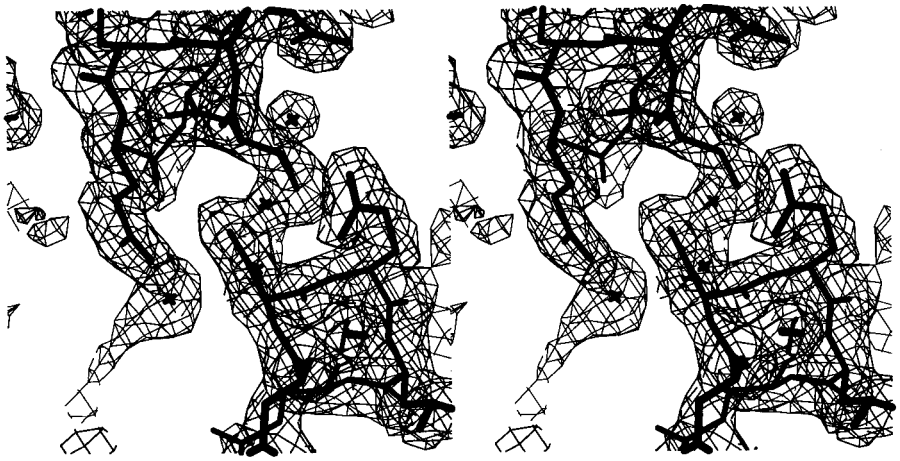

FIGURE 2: Electron density map (final $2F_o - F_c$ map contoured at 1σ) showing the contacts between two molecules in the asymmetric unit of the crystals with the intermolecular disulfide bridge in the center.

Table 2: Refinement Statistics

resolution (Å)	20−2.2
R (all data) (%)	23.2
R_{free} (10% data) (%)	29.6
rms deviations	
bond length (Å)	0.007
angle (deg)	1.8
no. of atoms	
protein	1833
H_2O	303
Ramachandran plot statistics (*41*)	
residues in the most favored regions (%)	91.4
residues in additionally allowed regions (%)	8.1
residues in generously allowed regions (%)	0.5

and angles are 0.01 Å and 1.8°, respectively. The rms deviation from planarity for all the aromatic groups is 0.007 Å. All residues that are visible in the electron density are in the allowed regions of the Ramachandran plot. Loop 67−72 is disordered in all four molecules in the asymmetric unit. Structure validation using the PROCHECK program (*41*) suggests that the goodness of the structure is within what is observed for structures refined at 2.2 Å resolution.

RESULTS AND DISCUSSION

The structure of flavin reductase was solved using multiple wavelength anomalous diffraction (MAD) on a gold derivative. Gold has been used for structure determination using MAD in only very few cases (*42*). The resulting electron density map was of good quality (Figure 2). The crystals contain four molecules in the asymmetric unit and were originally refined with noncrystallographic symmetry (NCS) which was released in the final stages. The present model is refined at 2.2 Å with an *R*-factor of 23.2% and an R_{free} of 29.6% (Table 2); it has good stereochemistry and all residues are in the allowed region of the Ramachandran plot. The final electron density map is of good quality; however, the loop of residues 67−72 has very weak density in all four molecules in the asymmetric unit indicating flexibility. Similarly, the two C-terminal residues have weak density.

Subunit Structure. The flavin reductase molecule is divided into two domains, an N-terminal domain that binds flavin (see below) and a C-terminal domain which probably is responsible for NAD(P)H binding (Figure 3). The N-terminal domain is dominated by a β-sheet sandwich of six strands

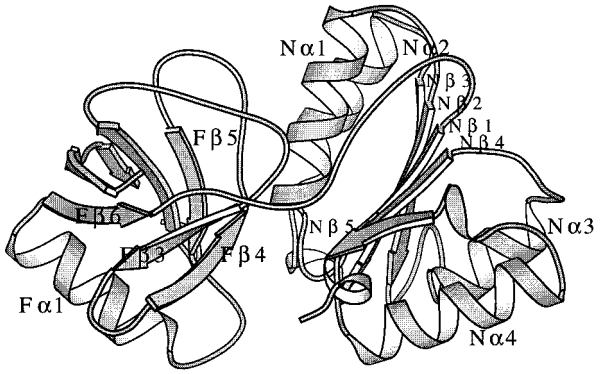

FIGURE 3: The flavin reductase molecule is divided into two domains, an N-terminal domain that binds riboflavin and a C-terminal domain that is analogous to structurally related enzymes and probably binds NAD(P)H. The secondary structure elements are numbered consecutively within each domain with the prefix F and N, respectively.

and contains one α-helix. One of the strands contains a *cis*-Pro peptide bond (Pro91) where the peptide oxygen forms a hydrogen bond to the N-terminus of the protein. The C-terminal domain is of α/β type with six strands and four helices. One of the strands at the edge of the molecule is very short, and only one residue is involved in the regular hydrogen bonding of the sheet. The C-terminal domain also contains three short 3_{10} helices.

The four molecules in the asymmetric unit are very similar, and the positions of the Cα atoms of these molecules deviate by 0.5−0.9 Å (Table 3). The positional differences between Cα atoms in the different domains of the four molecules are about 0.4 Å. The higher values for the whole molecules are due to small differences in relative domain orientation. Flavin reductase appears as a monomer in solution, but in the crystals the four molecules in the asymmetric unit form two dimers which are linked to each other by an intermolecular disulfide bridge between Cys149 from two molecules (Figure 4). This cysteine is located on the outside of the Nα2 helix, and there are a few other contacts between these molecules. The contacts in the crystal dimers are formed by homologous interactions between helices Nα3 and Nα4 from two molecules. In the center of this interaction area there are four hydrophobic residues from each subunit, Leu182, Leu186, Ile208, and Leu212, surrounded by hydrogen-bonded charged residues. This hydrophobic patch is probably

Table 3: Root Mean Square Differences for the Cα Atoms of the Four Molecules in the Asymmetric Unit and between Different Members in the Ferredoxin Reductase Superfamily, FNR, PDR, FlxR, NR, and B5R

	rms differences[a] (Å)		
	subunit	F-domain	N-domain
FreA−FreB	0.64 (232)	0.69 (98)	0.44 (133)
FreA−FreC	0.58 (232)	0.37 (98)	0.44 (133)
FreA−FreD	0.71 (232)	0.43 (98)	0.56 (133)
FreB−FreC	0.67 (232)	0.62 (98)	0.33 (133)
FreB−FreD	0.86 (232)	0.65 (98)	0.42 (133)
FreC−FreD	0.56 (232)	0.30 (98)	0.55 (134)
FreA−FNR spinach	1.59 (180)	1.36 (79)	1.71 (101)
FreA−FNR *Anabaena*	1.58 (171)	1.36 (79)	1.81 (97)
FreA−PDR	1.74 (171)	1.48 (81)	1.63 (89)
FreA−FlxR	1.82 (188)	1.61 (81)	1.61 (110)
FreA−NR1	1.91 (193)	1.67 (86)	1.68 (113)
FreA−NR2	1.96 (190)	1.72 (84)	1.90 (113)
FreA−B5R	2.00 (189)	1.84 (88)	1.63 (103)

[a] The number of Cα atoms used in the superposition is given within parentheses.

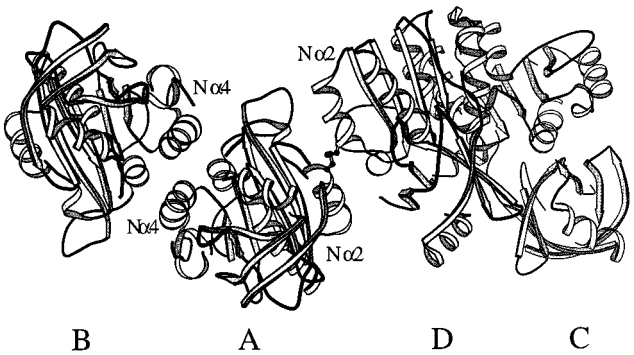

FIGURE 4: The four molecules in the asymmetric unit form two dimers which are linked to each other by an intermolecular disulfide bridge between Cys149 from helix Nα4 from two molecules (in the center of the figure). The dimerization is probably a result of the high protein concentration at crystallization. Monomers are usually detected in diluted solutions after purification. The interactions between molecules C and D are similar to those between molecules A and B.

responsible for the hydrophobic character of the enzyme as manifested in its affinity for phenyl-Sepharose columns (*2, 16*). A total of 957 Å^2 per subunit is buried upon dimer formation.

Comparison with Structures in the Ferredoxin Reductase Family. It is obvious from the structure that flavin reductase belongs to the ferredoxin reductase superfamily and shares overall structural features with other members (Figure 5). Despite very low sequence identity (about 15%), the domains are very similar to those of the ferredoxin reductase family. The secondary structure elements are practically the same, and about 75% of the residues in flavin reductase have equivalent residues in the other structures. Superpositioning of the ferredoxin reductase flavoproteins on flavin reductase can be achieved with an rms difference of 1.5−2.0 Å for about 180 Cα atoms. The relation between the domains differs only slightly from other members of the family. The most striking difference between flavin reductase and the flavoenzymes is that the loop between Fβ5 and Fα1 is much shorter than in most of the FAD binding flavoenzymes and there is no pronounced binding site for an AMP moiety of a FAD molecule (see below).

In a recent comparison of structures belonging to the superfamily (*30*), 10 residues were found to be conserved in all available three-dimensional structures. Of these, only four residues remain totally conserved in the structural family now including the flavin reductase structure: three glycines (residues 33, 111, and 201 in flavin reductase) and one arginine (residue 46 in flavin reductase) (Figure 1). Gly33 is located in the third position in an internal β-turn of type II, for which Gly is preferred for steric reasons. The residue is close to Tyr116 at the inside of the isoalloxazine binding site. From structural results of other members of the FNR family it seems plausible that Gly111 is in the center of the NADP(H) binding site and provides space for the pyrophosphate of the coenzyme and Gly201 is located at the nicotinamide binding site (*19*−*31*). The arginine, Arg46, is at the phosphate binding site for FAD and FMN and is conserved within the Fre enzymes but not in the LuxG enzymes.

Riboflavin Binding. The structure of flavin reductase was first solved in its unligated form. Soaking experiments were then performed to locate binding sites, and the binding of riboflavin has now been established. The electron density for the bound riboflavin is shown in Figure 6a, and its interactions with the protein are shown in Figure 6b,c. The corresponding binding site for FNR is also shown (Figure 6d). The isoalloxazine binding site is surrounded by hydrophobic residues, in particular several aromatic residues, but the binding site also contains a few polar residues and one aspartic acid. The inside of the isoalloxazine pocket is formed by Ser49, Ser115, and Tyr116. All other flavin reductases of the Fre and LuxG types have these residues. Two of the walls of the pocket also contain aromatic side chains, Tyr35 and Phe48 as well as Pro47, Asp227, and the main chain of residues 63−64 and 227−228. Ser49 is at the position to form a hydrogen bond to N5 of the isoalloxazine with its main chain amino group. At the O4 oxygen position of the isoalloxazine, flavin reductase has Ser115. Thr112 is close to the O2 oxygen atom, and Asp227 is close to the edge of the isoalloxazine ring where the methyl groups are. Phe203 and Phe231 are located at the top of the binding site. Flexible loop 65−72 is stabilized slightly by the binding of the riboflavin substrate.

Comparison between the Flavin Binding Site in Flavin Reductase and the Flavoenzymes in the Ferredoxin Reductase Family. Generally the isoalloxazine binding site of flavin reductase is most similar to the corresponding binding site in the other enzymes in the superfamily (Figure 6d), whereas the remaining parts of the FAD/FMN binding site differ such that the flavins can be released after reduction. The most striking difference between flavin reductase and most of the other members of the superfamily, such as FNR (*19, 22*), is that the loop responsible for the binding of the adenosine part of FAD is much shorter (Figure 5) and is disordered in the absence of flavin. The corresponding loop is also shorter in phthalate dioxygenase reductase (*28*) where the cofactor is FMN and in flavodoxin reductase (*30*) where FAD has an unusual twisted conformation and is bound by an extra Trp at the C-terminus of the NAD(P) domain. A similar FAD conformation was recently reported for FNR from *Azotobacter vinelandii* (*23*) where a phenylalanine stacks against the adenine ring.

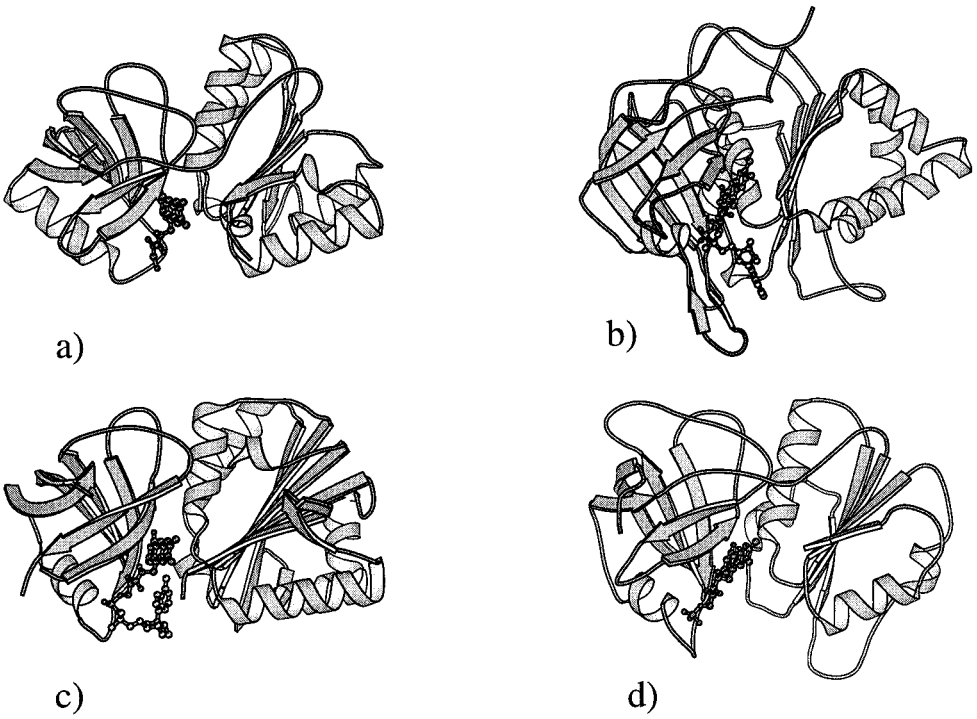

FIGURE 5: Structural comparison of (a) flavin reductase with bound riboflavin, (b) spinach ferredoxin with bound FAD, (c) *E. coli* flavodoxin reductase with bound FAD, and (d) phthalate dioxygenase reductase with bound FMN. The iron−sulfur domain is not included in the phthalate dioxygenase reductase structure.

(A) Isoalloxazine Site. The riboflavin binding site of flavin reductase is similar to the corresponding binding site in the ferredoxin reductase family and has a few features which are common to all enzymes in the superfamily. A glycine equivalent to Gly201 in flavin reductase is present in all reductases of the FNR superfamily. It probably provides space for the nicotinamide ring to come into contact with the isoalloxazine. The flavin site is hydrophobic in all enzymes with a number of aromatic residues which participate in flavin binding through hydrophobic and stacking interactions. All enzymes have an aromatic residue in contact with the *si* side of the isoalloxazine. In flavin reductase this residue is a Phe (residue 48), which is also found in most flavin reductases from other species instead of the more common Tyr in other enzymes (Figure 1). At the C7-methyl edge of the isoalloxazine binding site, flavin reductase differs from most other structures by having a tyrosine, Tyr35, where other structures have His, Asn, or Ser. Other flavin reductases of the Fre and LuxG types have an aromatic residue at this position, usually Tyr. An aromatic residue at this position should be favorable for isoalloxazine binding. The methyl groups were shown to contribute to the binding of the flavin as K_d values for methyl-free analogues were greatly increased (*16*). A proline, Pro47, at this edge of the isoalloxazine binding site is also present in all flavin reductases of the Fre and LuxG types but differs in most other structures. The inside of the isoalloxazine pocket contains a proline in all previously determined structures while flavin reductase has Tyr116. All other flavin reductases of Fre and LuxG types also have Tyr at this position.

A number of site-directed mutants of the ferredoxin−$NADP^+$ oxidoreductase from various species have been prepared for understanding the function of specific residues in enzyme structure, isoalloxazine binding, and catalysis. Ser96 in spinach FNR, which interacts with the N5 position of the FAD group, has been found to be a critical residue for catalysis (*19*−*21*). It is a serine in all FNRs and a serine or a threonine in all known family members. The Ser to Val mutation results in a 1000-fold decrease of the catalytic efficiency of the enzyme (*44*). In flavin reductase, Ser49 is found in the same stretch of residues, within the conserved RXXS(T) sequence, and in an equivalent structural position in the flavin site. Furthermore, this residue has been mutated to Thr or Ala (*43*). The first substitution had little effect on the K_m values and the activity of the enzyme. However, a Ser to Ala mutation resulted in a 500-fold decrease of the catalytic efficiency of the enzyme and a decreased affinity for the flavin. Both site-directed mutagenesis and structural characterization of flavin reductase lead to the conclusion that Ser49 is a critical residue in this class of enzymes.

At the polar edge of the isoalloxazine ring, N3 is in all structures of the family hydrogen bonded to a main chain carbonyl that has a similar position in flavin reductase. This is consistent with a decrease in the catalytic efficiency of the flavin reductase upon methylation of N3 (*16*). Some of the enzymes have a threonine binding to the O4 oxygen. Flavin reductase has Ser115 at this position. Thr112 is close to the O2 oxygen atom as in most structures but not hydrogen bonding.

Like most other members of the superfamily, flavin reductase also has a carboxylate side chain (Asp227) close to the edge of the isoalloxazine ring where the methyl groups are. All flavin reductases have Asp at this position while FNR has a Glu. In FNR, the catalytically important serine is hydrogen bonded to the carboxylate of a glutamate residue (Glu312 in spinach FNR and Glu301 in *Anabaena* FNR). Replacement of this residue with alanine resulted in significant decreases in the observed electron-transfer rate constant between the FNR and its substrates (*45*). It has been proposed that this residue, which is exposed to the solvent, might

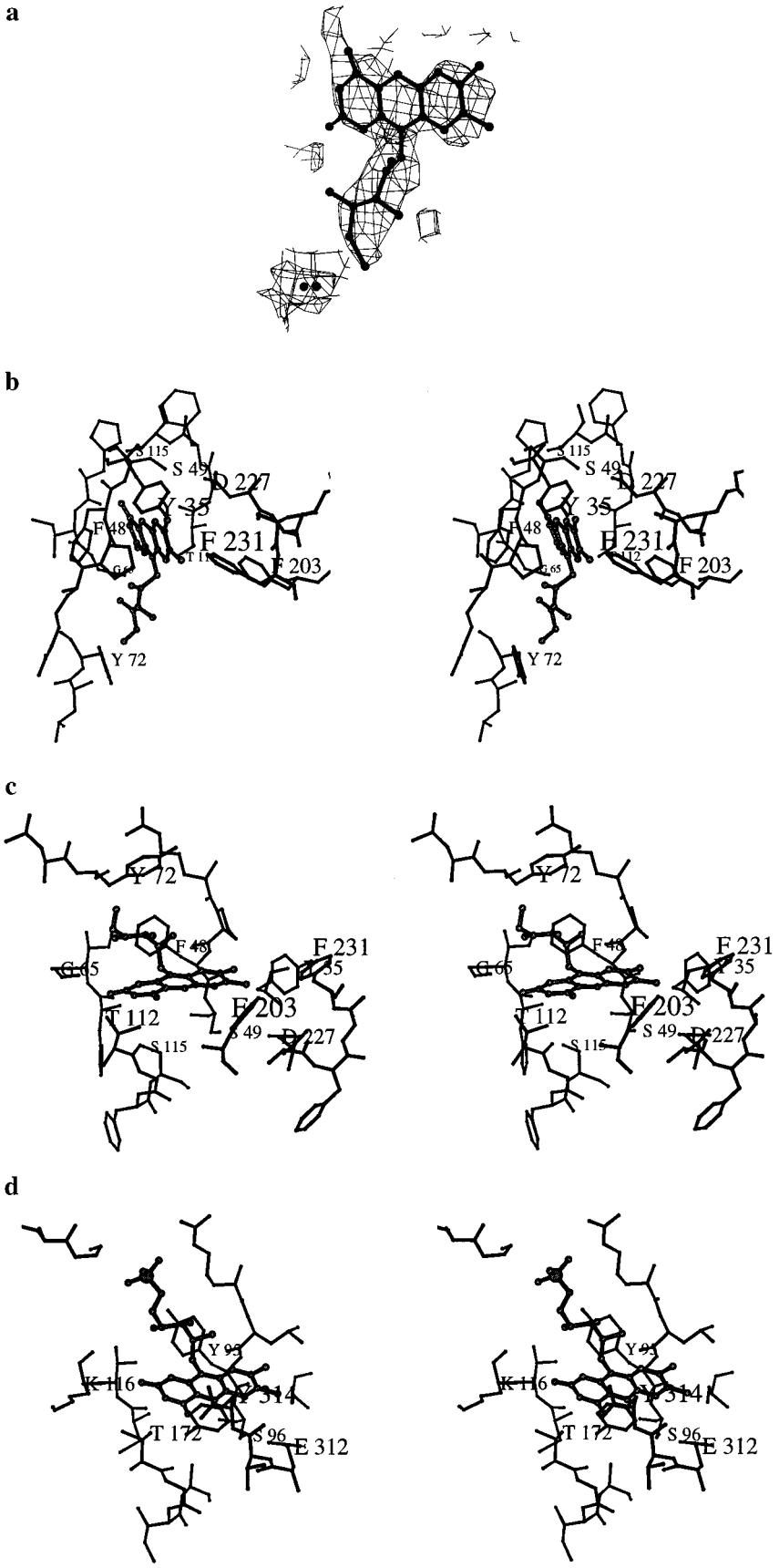

FIGURE 6: Isoalloxazine binding site of flavin reductase. (a) An omit $2F_o - F_c$ electron density map at 3.0 Å resolution contoured at 1σ of the riboflavin binding site. (b) Stereo picture of the riboflavin binding site. (c) Stereo picture of the riboflavin binding site viewed roughly along the riboflavin. (d) Stereo picture of the isoalloxazine binding site in spinach FNR (*19*) with the FMN part of FAD.

participate in proton transfers coupled to electron transfer during catalysis. In flavin reductase the structurally homologous aspartate points in the direction of the important Ser49 and is close to one edge of the isoalloxazine ring.

(B) Ribityl Binding Site. The ribityl moiety of the riboflavin forms only one direct hydrogen bond to the protein from O2′ to the carbonyl oxygen of Pro47. This is consistent with the experiments which show that riboflavin analogues lacking a 2′-OH were less efficiently reduced by flavin reductase (*16*). The ribityl binding site is slightly different from those in the flavoproteins of the ferredoxin reductase family. The flavoproteins have a conserved tyrosine that forms a hydrogen bond to the ribityl, whereas flavin reductase has a phenylalanine (residue 48) which can only provide van der Waals interactions for the isoalloxazine. All other flavin reductases also have phenylalanine in this position. Furthermore, an indirect hydrogen bond through a water molecule from a main chain nitrogen atom exists for most of the flavoenzymes of the superfamily. Pro47 in flavin reductase cannot provide such an interaction.

Altogether, from the structure of the riboflavin complex it appears that the contribution of ribityl to the binding of flavins should be smaller for flavin reductase than for the others. Considering the fact that modifications at the ribityl chain, except at the O2′ position, do not affect the binding of the flavin (*16*), it is very likely that these interactions take place with the aromatic isoalloxazine ring almost exclusively and provide the principal determinant for recognition and binding of the flavin moiety.

(C) Phosphate Binding Site. There is in the flavin domain of the flavoproteins of the ferredoxin reductase family only one helix, and this helix binds the phosphates of FAD or FMN at its amino end with direct or indirect hydrogen bonds. The corresponding helix in flavin reductase is longer and tilted about 20° and is less suitably oriented for phosphate binding. The main chain nitrogens are not pointing directly at the phosphate binding site. A conserved Arg in the FNR superfamily is involved in interactions with phosphates of FMN and FAD substrates. The contribution of the corresponding Arg46 to the FAD and FMN binding must be small since K_m values for FAD and FMN are comparable to those for riboflavin (*16*).

(D) Binding Site for the AMP Moiety of FAD. The difference in the flavin binding site with a very short loop between Fβ5 and Fα1 of flavin reductase (Figure 5) appears to be the main reason for the difference between the flavoenzymes of the superfamily and flavin reductase. For flavin reductase, the flavins are substrates and do not remain bound to the enzyme as for the others. The absence of the structural elements which interact with the ADP moiety of FAD is also consistent with the substrate specificity of the enzyme (*16*). The binding constants of FAD and FMN do not differ much from that of riboflavin.

(E) Stacking Residues. A common feature of the flavoenzymes of the ferredoxin reductase superfamily is that they have a residue in the C-terminus of the C-terminal domain that stacks against the isoalloxazine ring. This residue is thought to move away during the reaction and be substituted by the nicotinamide ring of the coenzyme. The presence of this stacking interaction is probably to protect the reduced flavin from side reactions. In the case of Fre, there are

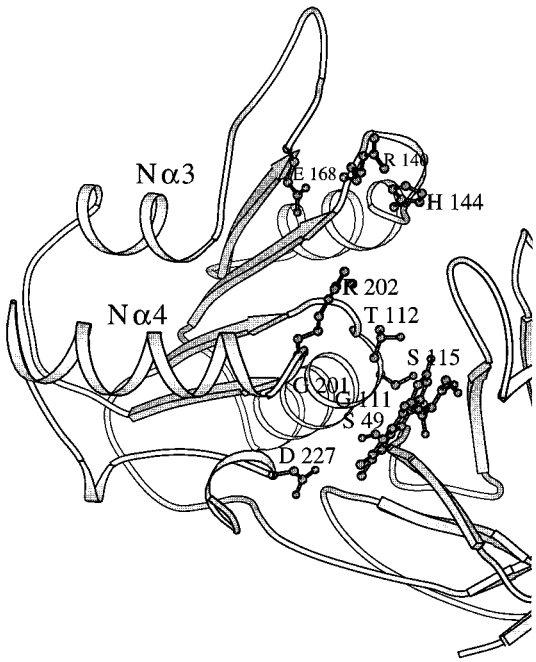

FIGURE 7: Proposed NAD(P)H binding site with residues implicated in NAD(P)H binding shown in ball-and-stick representation. The riboflavin molecule is also included to the right of the central helix.

aromatic residues at the isoalloxazine binding site but no residue that corresponds to the stacking position.

The role of the C-terminal tyrosine was investigated in the pea FNR enzyme (position 308 and position 314 in the spinach FNR) through the introduction of several substitutions (*46*). This residue is stacked coplanar to the *re* face of the isoalloxazine ring making extensive π-orbital contact with it and was suggested to fill the nicotinamide pocket in the absence of the nucleotide and thus protect the flavin. Only changes to nonaromatic side chains caused a major effect on the catalytic efficiency with large decreases of the k_{cat} values, without affecting the interaction with substrates. Phe229 or Phe231 at the C-terminus of flavin reductase might not play a similar role as no conformational change is observed in the riboflavin complex.

Plausible NAD(P)H Binding Site. The binding of NAD(P)H in a productive conformation is usually difficult to study for flavoenzymes and has only been successful for glutathione reductase where the stacking tyrosine moves away from its position in the absence of NADPH and the nicotinamide comes into the productive position (*47*). For flavin reductase no soaking experiment with NADPH or reduced nicotinamide mononucleotide NMNH has so far been successful despite several trials. For the ferredoxin reductase family, the NAD(P)H binding site has been mapped by binding studies in several cases (*19*, *22*, *27*, *48*), but it is essentially the ADP binding site that has been experimentally verified and the rest of the NAD(P)H binding site could be extended by model building to reach the isoalloxazine ring. The NAD(P)H binding site in flavin reductase can be extrapolated from analogy with these studies (Figure 7). The adenine ring should bind between the amino ends of helices Nα3 and Nα4. The ribose of an NAD molecule may bind to Glu168, which is in a position similar to that of Asp205 in the nitrate reductase−NADH complex. Alternatively, the 2′-phosphate group of NADPH may bind to Arg140 which is at the equivalent position as Arg176 in nitrate reductase

and the arginines in NADPH-dependent reductases. Alternatively, this arginine may turn and bind the pyrophosphate, which may also be bound by Arg202 and His144. The glycine-rich region with the conserved Gly111 makes space for the phosphates, Thr112 may bind the ribose, and the conserved Gly201 probably allows the nicotinamide to come into contact with the isoalloxazine. Asp227 may bind the carboxyamide of the nicotinamide. Even though the information on NAD(P)H binding is still limited in FNR and flavin reductase, it is very likely that the positioning of the isoalloxazine/NAD(P)H pair is the same in both systems, as shown from the detection of similar charge-transfer complexes during catalysis (*17*).

Evolution. It is tempting to assume that the structural design provided by flavin reductase for binding flavins and catalyzing their reduction by reduced pyridine nucleotides is one of the simplest solutions for this particular problem. Flavin−protein interactions involve the isoalloxazine ring almost exclusively (*16*) and are too weak to generate a flavoprotein. Furthermore, substrate specificities are broad with respect to both the flavin and the reduced pyridine nucleotide. As a consequence, flavin reductase behaves more as a general reducing system with no specificity for the electron acceptor since free reduced flavins, as small molecules, have the potential to transfer electrons to a large number of redox-active molecules. Flavin reductase is a primitive flavin-binding and flavin-reducing protein.

The requirement for more specific reactions has led to slight modifications of the structure and sequence of flavin reductase to generate a true flavoprotein with a tight interaction between the flavin and the polypeptide chain. Therefore, proteins such as FNR evolved. The transformation of flavin reductase into an FAD-containing FNR might be possible simply by the addition of a loop between positions 68 and 69 which provides specific residues for additional interactions with the ribose, the phosphates, and the adenine of FAD. The loop might not be as long as in the FNR from spinach or in cytochrome b_5 reductase, if some aromatic residues such as Trp are available at the C-terminus for providing a stacking interaction to the adenine, as shown in the case of the flavodoxin reductase from *E. coli*, or if FMN, instead of FAD, is the selected flavin prosthetic group, as in phthalate dioxygenase reductase. Additional modifications served to make specific contacts to electron acceptors, such as ferredoxin and cytochrome b_5.

The third step of evolution of the flavin reductase unit corresponded to the addition to the FNR protein of a second unit, most probably by gene fusion mechanisms (*20*). This generated enzymes such as phthalate dioxygenase reductase or the reductase component of methane monooxygenase by addition of a ferredoxin unit, cytochrome P450 reductase or sulfite reductase by addition of a FMN−flavodoxin unit, or flavocytochrome *b*-245 (*49*) by addition of a heme domain. All these proteins could be further complicated by addition of a third unit, a Mo−pterin to a flavocytochrome in nitrate reductase or a heme domain to a FAD + FMN flavoprotein in NO synthase. It is noteworthy that in these systems the three-dimensional structural arrangement of the flavin reductase domains has been conserved, even though during evolution the sequences were greatly modified with only three residues conserved (Figure 1).

Flavin Reductase Family. While very few residues are conserved within the ferredoxin reductase superfamily, the conservation of sequence within the flavin reductase family is much larger. As much as 50 residues (about 20% of the residues) are strictly conserved within the family. These are clustered around the isoalloxazine and proposed NAD(P)H binding sites but also the hydrophobic cores of the flavin reductases are to a large extent conserved. This indicates that the three-dimensional structures of all these flavin reductases are very similar. The overall sequence similarities to *E. coli* flavin reductase for the other flavin reductases are between 36% and 73% identities.

ACKNOWLEDGMENT

We thank Vivian Stajnoff, ESRF, Grenoble, for help in data collection and Irmgard Kurland for linguistic corrections.

REFERENCES

1. Fontecave, M., Coves, J., and Pierre, J. L. (1994) *BioMetals 7*, 3−8.
2. Fontecave, M., Eliasson, R., and Reichard, P. (1987) *J. Biol. Chem. 262*, 12325−12331.
3. Fontecave, M., Eliasson, R., and Reichard, P. (1989) *J. Biol. Chem. 264*, 9164−9170.
4. Fontecave, M., Gerez, C., Mansuy, D., and Reichard, P. (1990) *J. Biol. Chem. 265*, 10919−10924.
5. Coves, J., Delon, B., Climent, I., Sjöberg, B. M., and Fontecave, M. (1995) *Eur. J. Biochem. 233*, 357−363.
6. Quandt, K. S., and Hultquist, D. E. (1994) *Proc. Natl. Acad. Sci. U.S.A. 91*, 9322−9326.
7. Nagai, M., Mawatari, K., Nagai, Y., Horita, S., Yoneyama, Y., and Hori, H. (1995) *Biochem. Biophys. Res. Commun. 210*, 483−490.
8. Chikuba, K., Yubisui, T., Shirabe, K., and Takeshita, M. (1994) *Biochem. Biophys. Res. Commun. 198*, 1170−1176.
9. Tu, S. C., and Mager, H. I. X. (1995) *Photochem. Photobiol. 62*, 615−624.
10. Kendrew, S., Harding, S., Hopwood, D., and Marsh, E. (1995) *J. Biol. Chem. 270*, 17339−17343.
11. Parry, R. J., and Li, W. (1997) *J. Biol. Chem. 272*, 23303−23311.
12. Blanc, V., Lagneaux, D., Didier, P., Gil, P., Lacroix, P., and Crouzet, J. (1995) *J. Bacteriol. 177*, 5206−5214.
13. Xu, Y. R., Mortimer, M. W., Fisher, T. S., Kahn, M. L., Brockman, F. J., and Xun, L. Y. (1997) *J. Bacteriol. 179*, 1112−1116.
14. Gray, K. A., Pogrebinsky, O. S., Mrachko, G. T., Xi, L., Monticello, D. J., and Squires, C. H. (1996) *Nat. Biotechnol. 14*, 1705−1709.
15. Gaudu, P., Touati, D., Nivière, V., and Fontecave, M. (1994) *J. Biol. Chem. 269*, 8182−8188.
16. Fieschi, F., Nivière, V., Frier, C., Decout, J. L., and Fontecave, M. (1995) *J. Biol. Chem. 270*, 30392−30400.
17. Nivière, V., Vanoni, M. A., Zanetti, G., and Fontecave, M. (1998) *Biochemistry 37*, 11879−11887.
18. Spyrou, G., Haggard-Ljungquist, E., Krook, M., Jörnvall, H., Nilsson, E., and Reichard, P. (1991) *J. Bacteriol. 173*, 3673−3679.
19. Karplus, P. A., Daniels, M. J., and Herriott, J. R (1991) *Science 251*, 60−66.
20. Karplus, P., and Bruns, C. M. (1994) *J. Bioenerg. Biomembr. 26*, 89−99.
21. Bruns, C. M., and Karplus, P. A. (1995) *J. Mol. Biol. 247*, 125−145.
22. Serre, L., Vellieux, F. M. D., Medina, M., Gomez-Moreno, C., Fontecilla-Camps, J. C., and Frey, M. (1996) *J. Mol. Biol. 263*, 20−39.
23. Sridhar Prasad, G., Kresge, N., Muhlberg, A. B., Shaw, A., Jung, Y. S., Burgess, B. K., and Stout, C. D. (1998) *Protein Sci.7*, 2541−2549.

24. Nishida, H., and Miki, K. (1996) *Proteins: Struct. Funct. Genet. 26*, 32−41.
25. Nichida, H., Inaka, K., Yamanaka, M., Kaida, S., Kobayashi, K., and Miki, K. (1995) *Biochemistry 34*, 2763−2767.
26. Lu, G., Campbell, W. H., Schneider, G., and Lindqvist, Y. (1994) *Structure 2*, 809−821.
27. Lu, G., Lindqvist, Y., Schneider, G., Dwivedi, U., and Campbell, W. (1995) *J. Mol. Biol. 248*, 931−948.
28. Correll, C. C., Batie, C. J., Ballou, D. P., and Ludwig, M. L. (1992) *Science 258*, 1604−1610.
29. Correll, C. C., Ludwig, M. L., Bruns, C. M., and Karplus, P. A. (1993) *Protein Sci. 2*, 2112−2133.
30. Ingelman, M., Bianchi, V., and Eklund, H. (1997) *J. Mol. Biol. 268*, 147−157.
31. Wang, M., Roberts, D., Paschke, R., Shea, T., Masters, B., and Kim, J. (1997) *Proc. Natl. Acad. Sci. U.S.A 94*, 8411−8416.
32. Otwinowski, Z. (1993) *Proceedings of the CCP4 study weekend*, pp 56−62, Daresbury Laboratory, Warrington, U.K.
33. CCP4 (1994) *Acta Crystallogr. D50*, 760−763.
34. de La Fortelle, E., and Bricogne, G. (1997) *Methods Enzymol. 276*, 442−494.
35. Abrahams, J. P., and Leslie, A. G. W. (1996) *Acta Crystallogr. D52*, 30−42.
36. Cowtan, K. (1994) *Joint CCP4 and ESF-EACBM Newsletter on Protein Crystallography* Vol. 31, pp 34−38, Daresbury Laboratory, Warrington, U.K.
37. Jones, T. A., Zou, J. Y., Cowan, S. W., and Kjeldgaard, M. (1991) *Acta Crystallogr. 47*, 110−119.
38. Murshudov, G. N., Vagin, A. A., and Dodson, E. J. (1997) *Acta Crystallogr. D53*, 240−255.
39. Navaza, J. (1994) *Acta Crystallogr. 50*, 157−163.
40. Lamzin, V. S., and Wilson, K. S. (1993) *Acta Crystallogr. D49*, 129−147.
41. Laskowski, R. A., MacArthur, M. W., Moss, D. S., and Thornton, J. M. (1993) *J. Appl. Crystallogr. 26*, 283−291.
42. Ogata, C. M. (1998) *Nat. Struct. Biol. 5*, 638−640.
43. Nivière, V., Fieschi, F., Decout, J. L., and Fontecave, M. (1996) *J. Biol. Chem. 271*, 16656−16661.
44. Aliverti, A., Bruns, C., Pandini, V., Karplus, P., Vanoni, M., Curti, B., and Zanetti, G. (1995) *Biochemistry 34*, 8371−8379.
45. Medina, M., Martinez-Julvez, M., Hurley, J., Tollin, G., and Gomez-Moreno, C. (1998) *Biochemistry 37*, 2715−2728.
46. Orellano, E. G., Calcaterra, N. B., Carillo, N., and Ceccarelli, E. A. (1993) *J. Biol. Chem. 268*, 19267−19273.
47. Mittl, P., Berry, A., Scrutton, N., Perham, R., and Schulz, G. (1994) *Protein Sci. 3*, 1504−1514.
48. Correll, C. C., Ludwig, M. L., Bruns, C. M., and Karplus, P. A. (1993) *Protein Sci. 2*, 2112−2133.
49. Segal, A. W., West, I., Wientjens, F., Nugent, J. H. A., Chavan, A. J., Haley, B., Garcia, R. C., Rosen, H., and Scrace, G. (1992) *Biochem. J. 284*, 781−788.

BI982849M